Transilvania University of Brasov
FACULTY OF MECHANICAL ENGINEERING
ICMSAV2018 & COMAT2018 & eMECH2018
Brasov, ROMANIA, 25-26 October 2018

ON THE SONOELASTICITY AND SONIFICATION IMAGING THEORIES WITH APPLICATION TO COOPERATIVE SURGICAL ROBOTS

Cristian Rugina, Cristina Stirbu
Institute of Solid Mechanics, Romanian Academy, Bucharest, ROMANIA, rugina.cristian@gmail.com, cristina.stirbu29@gmail.com

Abstract : *Sonoelasticity imaging uses low-frequency vibrations in tissue and Doppler vibration pattern to detect small inhomogeneities in tissues. The sonification theory translates the tissue data into acoustic signals and reverses back the sound into images by solving an inverse problem. In contrast to sonoelasticity which is limited to low examination frequencies imposed by the high attenuation of acoustic waves, the sonification theory is extending the range of frequencies to areas of medical interest. In addition, sonoelasticity is limited to detection of only small inhomogeneities in tissue due to the Born approximation, while the sonification theory is extending to detect the tumors of different sizes. Fundamental theoretical considerations of both theories are reviewed in this paper with application to cooperative surgical robots. For implementing an effective control, detailed images of the tumor and its neighboring regions are required.*
Keywords : *Dopler, Elasticity, Vibration, Sonification.*

1. INTRODUCTION

Sonoelasticity imaging uses low-frequency (100-Hz) vibrations in tissue and Doppler imaging of vibration patterns to detect and define hard tumors. A low frequency vibration is applied to excite internal vibrations within tissue. The inhomogeneity in a surrounding elastic region appears as a disturbance to the normal vibration eigenmode pattern. With applied stimulus by sinusoidal steady state vibrations, a production of modal patterns in tissues is obtained and the Doppler detection of vibration is followed by image generation [1-5]. Lerner and Parker pioneered this combination of externally applied vibration and new Doppler imaging techniques [6].
The sonification translates the set of data points into acoustic signals [7-10]. An important issue in this direction is the reversing back the sound samples into new data points in order to gain in clarity and contrast in medical images, and discovery of the hidden details in the tissue by reducing the noise [11,12].
In contrast to sonoelasticity, which is limited to low examination frequencies, the sonification theory is extending the range of frequencies to medical imaging interest, and in addition, it is extending to detect the tumors of different sizes. Sonoelasticity is limited to detection of only small inhomogeneities in tissue due to the Born approximation adopted in the propagation equations. The sonification takes advantage to detect hard tumors by identification of flaw position, size and depth. As other methods, namely vibro-thermography and thermoelastic emission for NDE of composite materials, both theories the sonoelasticity and sonification are practical and can be performed in situ.
Fundamental features of sonoelasticity and sonification imaging theories are reviewed in this article, with accent to the image prediction for hard tumor in a background of softer elastic tissue.
These approaches are exercised for delivering detailed images of the tumor and its neighboring regions required for an efficient control of motion of the surgical instrument for a cooperative surgeon-robot hybrid system. The task of the hybrid cooperation is to stop the surgical instrument to reach some forbidden frontiers.

2. SONOELASTICITY THEORY

The tumor is modelled as an elastic inhomogeneity inside a loss homogeneous elastic medium. The body occupies a 3D domain Ω, bounded by Γ. An inhomogeneity Ω_0 around the point (x_1^0, x_2^0, x_3^0) is presented into medium. The motion equation for a general linear and isotropic material is [13]

$$\frac{E(x)}{2(1+\nu)}\nabla^2 u + \frac{E(x)}{2(1+\nu)(1-2\nu)}\nabla\nabla u = \rho(x)u_{,tt}, \qquad (1)$$

where $x=(x_1,x_2,x_3)\equiv(x,y,z)$, $u(x,t)$ the displacement vector of components u_i, $i=1,2,3$, ρ mass density of material, $E(x)$, and ν are the Young's modulus and Poisson's ratio respectively.

Suppose that a vibration source is on the boundary $\Gamma_0\subset\Gamma$. The boundary conditions are

$$u(x',t)=0,\ x'\in\Gamma/\Gamma_0,\ \ u(x',t)=A_0\exp(\mathrm{i}\omega_0 t)\ f_0(x'),\ \ x'\in\Gamma_0, \tag{2}$$

where $x'=(x_1,x_2)$, ω_0 is the angular frequency, A_0 a constant, and f_0 a given function. Consider that the medium Young's modulus is a constant E_0, except the small domain Ω_0 around (x_0,y_0,z_0) has the Young's modulus E_0+E'. The displacement vector u can be decomposed into longitudinal and shear components in accordance to Helmholtz theorem $u=\nabla\varphi+\nabla\times\psi$. From (1) we obtain the Helmholtz equations

$$c_L^2\nabla^2\varphi=\ddot{\varphi},\quad c_T^2\nabla^2\psi=\ddot{\psi}, \tag{3}$$

where $c_L^2=\dfrac{\lambda+2\mu}{\rho}=\dfrac{E}{2\rho(1+\nu)(1-2\nu)}$ and $c_T^2=\dfrac{\mu}{\rho}=\dfrac{E}{2\rho(1+\nu)}$, are the longitudinal and transversal (shear) wave velocities. Next, we concentrate on shear waves, since low-frequency longitudinal waves have wavelengths that are too large compared to organs of interest at the frequencies used in sonoelasticity imaging [1]

$$c_T^2\nabla^2 u=\ddot{u}, \tag{4}$$

where c_T is given by

$$c_T^2(x)=\frac{E(x)}{2\rho(1+\nu)}=\frac{E_0+E'(x)}{2\rho(1+\nu)}=\frac{(1+E'(x)/E_0)E_0}{2\rho(1+\nu)}. \tag{5}$$

If denote $c_0^2=E_0/(2\rho(1+\nu))$, $\gamma(x)=E'(x)/E_0$, it follows in virtue of (4)

$$c_T^2(x)=c_0^2(1+\gamma(x)),\ \ \gamma(x)=\begin{cases}E'/E & \text{for}\quad \Omega_0,\\ 0 & \text{for}\quad \Omega/\Omega_0.\end{cases} \tag{6}$$

So, instead of writing two shear wave equations for both the homogeneous and inhomogeneous region, we may write one equation for the entire medium

$$c_0^2(1+\gamma(x))\nabla^2 u=\ddot{u}, \tag{7}$$

Since the medium is characterized by attenuation of waves, we introduce in (3.4) a relaxation term

$$\nabla^2 u-\frac{1}{c_0^2}\ddot{u}-\frac{R}{\rho c_0^2}\dot{u}=0, \tag{8}$$

where R is the mechanical resistance, defined by the equation $F_{\text{damping}}=-Rv$, with v the velocity.

The motion equation (8) becomes for $u=u\exp(\mathrm{i}\omega_0 t)$ and $K=\omega_0/c_0$ the wave number

$$\nabla^2 u+\frac{K^2}{(1+\gamma(x,y))}u-\frac{iK^2}{Q_0(1+\gamma(x,y))}u=0, \tag{9}$$

The displacement is the sum between the incident and scattered waves $u=u_{inc}+u_s$. For the quality factor at the angular frequency ω_0, $Q_0=\dfrac{\omega_0\rho}{R}$, the equation (9) becomes

$$\nabla^2 u_s+K^2u_s-\frac{\mathrm{i}K^2}{Q_0}u_s=\beta(x,y)K^2(1-\mathrm{i}/Q_0)(u_{inc}+u_s),\ \ \beta(x,y)=\begin{cases}\gamma/(1+\gamma) & \text{for } \Omega_0,\\ 0 & \text{for } \Omega/\Omega_0.\end{cases} \tag{10}$$

To simplify (10) the Born approximation is considered, i.e. the scattered wave is much smaller that the incident wave and therefore, the term $\beta(x,y)K^2(1-\mathrm{i}/Q_0)u_s$ can be discarded.

2. DIRECT SONIFICATION

For the beginning, we present the direct problem of sonification as it is known in the literature [12, 15-18].

The sonification operator is a bijective and reversible function at least when the data is in the digital range prior to D/A conversion. Each sample of sound can contain false characteristics because of the band-limited interpolation of the algorithm.

The ideal sound signal has auditory gestalts within time and frequency ranges withe good perceptibility for the listener. Thus, pure sonification is a compromise between the macroscopic temporal scale and the frequency range of the information.

The sonification operator S^0 transforms the point data space D into the sound signals space Y^0

$S^0 : D \to Y^0$, $S^0 : x(t) \to y^0(t^0, x(t), p^0)$, (11)

where $x(t)$ is the 1D point data to be transformed into sounds depending of the data time t, t^0 is the sonification time, and $p^0 \subseteq P^0$ where $P^0 = \{k^0, \Delta^0, f_{ref}^0, \alpha^0, \beta^0, \phi^0, \varepsilon^0, g^0, \gamma^0, H^0\}$. The parameters of P^0 are: k^0 the time compressor factor with the sonification time interval $T^0 = T / k^0, \Delta^0 \geq 0$ the dilation factor, f_{ref}^0 is the reference frequency, $\alpha^0, \beta^0 \geq 0$ the pitch scaling parameters, $\phi^0 \geq 1$ the power distorsion factor, $\varepsilon^0 \geq 0$ the threshold for the amplitude, g^0 the gain function, γ^0 the decay parameter and H^0 the timbral control function.
The one-dimensional data stream $x(t)$ can be divided into non-overlapping segments of different length, depending on application. For example, for the short-term fluctuation of a given information, the segments are built from the actual data with a moving average. The general form for the sonification signal $y^0(t^0)$ is

$$y_i^0(t^0) = | x_i(\Delta^0 t^0) | \sin\left(2\pi \int_0^{t^0} f_{ref}\, 2^{(x_{trend}(t_{i-1}) + x_i(\Delta^0 t^{0'}))} \mathrm{d}t^{0'} \right), \quad (12)$$

where the second term $x_i(\Delta^0 t^{0'})$ is the mean free segment, and $x_{trend}(t_{i-1})$ the trend signal at the starting point for pitch modulation. Parameter Δ^0 determine the length of the sonic event T_i^0 function on T_i If $\Delta^0 = k^0$ adjacent events do not overlap but for $\Delta^0 \leq k^0$ they overlap.
To introduce control of timbre, the operator H^0 acts as the sine function, so

$$y_i^0(t^0) = a_i(t^0) H^0 < \sin\left(2\pi \int_0^{t^0} f_{ref}\, 2^{b_i(t^{0'})} \mathrm{d}t^{0'} \right) >, \; b_i(t^{0'}) = \left(\alpha^0 x_{trend}(t_{i-1}) + \beta^0 x_i(\Delta t^{0'}) \right), \quad (13)$$

where $a_i(t^0)$ is the amplitude modulator, f_{ref} is the base frequency for the pitch range of sonification and $b_i(t^0)$ is a pitch modulator. The amplitude modulator is defined as

$$a_i(t^0) = | x_i(\Delta^0 t^0 |^{\phi^0}, \; \phi^0 \geq 1, \quad (14)$$

where φ^0 has the role of amplitude modulator.

2. NEW SONIFICATION OPERATOR

Let us to consider 3D digital image B seen as a collection of N pixels or dots seen as the smallest controllable element of a picture. We suppose that B is embedded in Euclidean space E^3, has the volume Ω_1 and surface Γ. A Cartesian coordinates X_K, $K = 1,2,3$ is taken as a reference frame at time $t = 0$, to locate a pixel $P \in B$ in Ω_1. The B forms N-dimensional set of data $D = \{d_1, d_2, ..., d_N\}, d_i \in R^N$ [12].
The B may be subjected to external force vector $f(t)$ written as the sum of the excitation harmonic force $F_p(t)$ and the generation sound force $F_s(t)$. The last force is introduced to build the sonification operator.
Given a known primary force vector F_p we want to determine the unknown function F_s such that the acoustic power radiated from B is a minimum.
B may occupy at a later time t a new configuration $b \in E^3$ with position vector of Cartesian coordinates x_k, $k = 1,2,3$. The response of B to the force vector f is a configuration b defined by the motion of a point $P \in B$ at time t. At frequency ω the velocity can be written in complex notation $v(t) = V \exp(\mathrm{i}\omega t)$. Similarly, the force is $f(t) = F \exp(\mathrm{i}\omega t)$. The response of B is written in terms of the complex mobility matrix (inverse of impedance) $\Sigma(\omega, \omega_j, \phi_j, \eta_j) = v(\mathrm{i}\omega) / f(\mathrm{i}\omega)$, $j = 1,2,...,M$ as [19]

$$v = \Sigma F, \quad (15)$$

where v is the velocity vector, F the point-force vector exciting B normal to Γ. The index j refers to the j vibration mode, ω is the harmonic excitation frequency, ω_j is the j th natural frequency, η_j is the damping loss factor associated with the j th natural frequency and ϕ_j is the mass normalized modal displacement vector perpendicular to Γ in air. The acoustic power radiated from B is written as

$$W = \frac{1}{2} v^T A v, \quad (16)$$

with v the velocity vector and A the acoustic impedance which is positive definite and Hermitian matrix, written in term of its M eigenvalues $\Lambda = \mathrm{diag}(\lambda_1, \lambda_2, ..., \lambda_M)$ and eigenvectors $Q = [q_1, q_2, ..., q_M]$

$$A = \sum_{i=1}^{M} \lambda_i q_i q_i^T \cdot \tag{17}$$

By substituting (15) in (16) we have

$$W = \frac{1}{2} F^T \Sigma^T (Q \Lambda Q^T) \Sigma F \,, \tag{18}$$

where the superscript T refers to Hermitian transpose conjugate operation.
By setting

$$\frac{\partial W}{\partial F_s} = 0 \,, \tag{19}$$

we determine the functions F_s under the form

$$F_s(d_j) = \mathrm{cn}(m_j, k_{1j} x_1 + k_{2j} x_2 + k_{3j} x_3 - \omega_j t + \tilde{\phi}_j) \,, \tag{20}$$

where n is the finite number of degrees of freedom of the cnoidal functions, $0 \le m_j \le 1$ is the modulus of the Jacobean elliptic function, ω_j are frequencies and $\tilde{\phi}_j$ the phases , k_{1j}, k_{2j}, k_{3j} are components of the wave vector [20].
The sonification operator $\Psi(D,t) : \Omega_1 \times T_0 \to \Omega_2 \times \overline{T}_0$ transforms dataset D to M -dimensional sound signal, where Ω_2 is a subset of R^n representing the sound domain, T_0 is the interval of time associated to D , and $\overline{T}_0$ is associated to Ω_2 . This operator is defined as

$$\psi(D,t) = \sum_{j=1}^{N} \left(\beta_j F_s(d_j) + \frac{\gamma_j F_s(d_j)}{1 + \zeta_j F_s(d_j)} \right), \tag{21}$$

where β_j , γ_j, ζ_j , $j = 1, 2, ..., n$, are parameters that are determined from a genetic algorithm.
The inverse sonification operator is given by

$$\Psi^{-1}(D) = \tilde{d} \,, \tag{22}$$

where $\Psi^{-1}(D) : \Omega_2 \times T_0 \to \Omega_1 \times T_0$, and $\tilde{d}$ the new image $\tilde{D} = \left\{ \tilde{d}_1, \tilde{d}_2, ..., \tilde{d}_N \right\}, \tilde{d}_i \in R^N$.
By applying the inverse sonification algorithm, a new digital image is obtained. We expect to obtain superior properties of new picture in comparison to the original one in terms of clarity, contrast and noise. In addition, new hidden details are expected to be discovered.

3. APPLICATION TO MEDICAL IMAGES

The control of robotic surgery systems consists in preventing the surgeon-tool to cross the vascular vessels in the tumor vicinity and depends on the quality of medical images of the tumor and its neighboring regions [21, 22].
The case of a tumor (pink color) located near the portal tree of the vascular territory is considered (Figure 1 and Figure 2). The image obtained by applying the sonoelasticity imaging was obtained by Gheorghe et al. [23] (Figure 3). The tumor is colored in blue.
The distinction between the hard and soft tissues is shown in nuances blue to red. The conclusion drawn from [23] is that the image distinguishes between benign and malignant tissues, and the diagnostic accuracy of the image is more correctly for colorful than for gray-scale images.
Also, the authors conclude that by refining selection of the tissue region, and by a larger number of images for each patient, the performance of real-time sonoelasticity imaging should be further improved.
The inverse sonification three images are shown in Figure 4, for the frontal, caudal and cranial views. Compared to sonoelasticity imaging, several benefits are reported by the inverse sonification technique.
Besides new details on the tumor reported to surrounding areas, the best views were found from which the shape and size of the tumor is better visualized.

Figure 1: Location of the tumor.

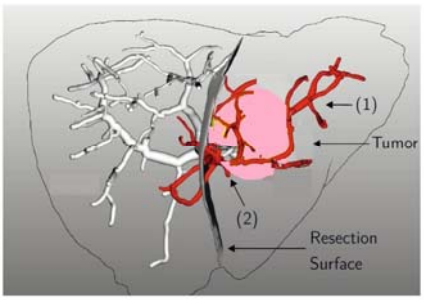

Figure 2: Vascular territory (1) and the vessel branches in the vicinity of tumor (2).

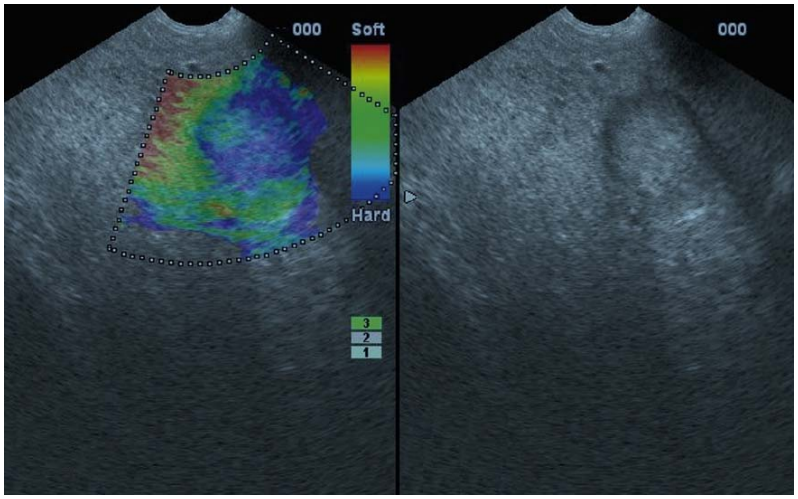

Figure 3: The sonoelastic image of the tumor [23].

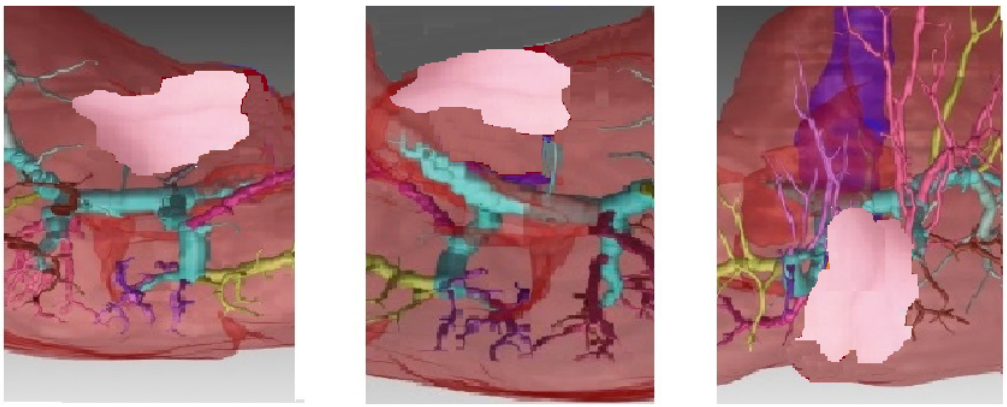

Figure 4 : Inverse sonification image in the vicinity of the tumor.

4. CONCLUSION

This paper reviews the fundamental features of sonoelasticity and sonification imaging theories with accent to the image prediction for hard tumor in a background of softer elastic tissue. Sonoelasticity imaging uses low-frequency vibrations in tissue and Doppler vibration pattern to detect small inhomogeneities in tissues. The sonification theory translates the tissue data into acoustic signals and reverses back the sound into images by solving an inverse problem. The inverse sonification problem has a remarkable property by improving the spatial resolution, contrast and noise of the medical image, and completing it with details that did not exist before. By comparing the old image with the new one, the results are surprising in that new hidden details are discovered.
These approaches are exercised to control the motion of the surgical instrument for a cooperative surgeon-robot hybrid system. The task of the hybrid cooperation is to stop the surgical instrument to reach some forbidden

frontiers. For implementing an effective control, detailed images of the tumor and its neighboring regions are required.

Acknowledgement: This work was supported by a grant of the Romanian ministry of Research and Innovation, CCCDI - UEFISCDI, project number PN-III-P1-1.2-PCCDI-2017-0221 / 59PCCDI/2018 (IMPROVE), within PNCDI III.

REFERENCES

[1] Gao, L., Parker, K.J., Alam, S.K., Lerner, R.M., Sonoelasticity imaging: theory and experiment verification, J. Acoust. Soc, Am., 97, 3875-3886, 1995.
[2] Gao, L., Sonoelastography: Theory and experiment development, PhD thesis, University of Rochester, NY, 1995.
[3] Gao, L., Parker, K.J., Alam, S.K., Lerner, R.M., Theory and application of sonoelasticity imaging, Sonoelasticity imaging: theory and experiment verification, Int. J. Imaging Syst. Technol., 8, 104–109, 1997.
[4] Chiroiu, V., Chiroiu, C., Inverse problems in mechanics (in Romanian). Ed. Academiei, Bucharest; 2003.
[5] Chiroiu, V., Chiroiu, C., Rugina, C., Delsanto, P.P., Scalerandi, M., Propagation of ultrasonic waves in nonlinear multilayered media, Journal of Computational Acoustics, 9(4),1633–1646, 2001.
[6] Lerner, R.M., Parker, K.J., Holen, J., Gramiak, R., Waag, R.C., Sonoelasticity: Medical Elasticity Images Derived from Ultrasound Signals in Mechanically Vibrated Targets. Acoustical Imaging, 16, 317–327, 1988.
[7] Kramer, G., An introduction to auditory display. In G. Kramer (Ed.), Auditory display: Sonification, audification, and auditory interfaces (pp. 1-78). Reading, MA: Addison Wesley, 1994.
[8] Kramer, G., Walker, B.N., Bonebright, T., Cook, P., Flowers, J., Miner, N., The Sonification Report: Status of the Field and Research Agenda. Report prepared for the National Sci. Foundation by International Community for Auditory Display. SantaFe, NM: International Community for Auditory Display (ICAD), 1999.
[9] Roodaki, H., Navab, N., Eslami, A., Stapleton, C., Navab, N., Sonifeye: Sonification of visual information using physical modeling sound synthesis, IEEE Trans. Vis. Comput. Graphics, 23(11), 2366–2371, 2017.
[10] Walker, B.N., Magnitude estimation of conceptual data dimensions for use in sonification, Journal of Experimental Psychology: Applied, 8, 211-221, 2002.
[11] Munteanu, L., Ioan, R., Majercsik, L., On the computation and control of a robotic surgery hybrid system, ICMSAV201818, Brasov, 25-26 Oct .2018.
[12] Chiroiu, V., Dragne, C., Gliozzi, A., On the trajectories control of a hybrid robotic system, ICMSAV201818, Brasov, 25-26 Oct. 2018.
[13] Landau L D, Lifshitz E M. Theory of elasticity. (3rd. edition) Pergamon Press: Oxford, U.K; 1986.
[14] Morse, P.M., Ingard, K.U., Theoretical Acoustics, McGraw-Hill, New York; 1968.
[15] Bonebright, T., Cook, P., Flowers, J.H., Sonification Report: Status of the Field and Research Agenda, Faculty Publications, Department of Psychology, Paper 444, 2010.
[16] Holdrich, R., Vogt, K., Augmented audification, in ICAD 15: Proceedings of the 21st International Conference on Auditory Display, K. Vogt, A. Andreopoulou, and V. Goudarzi, Eds. Graz, Austria:
Institute of Electronic Music and Acoustics, Univ. Music and Performing Arts Graz (KUG), 2015, pp. 102–108.
[17] Vickers, P., Holdrich, R., Direct segmented sonification of characteristic features of the data domain, preprint, Department of Computer and Information Sci., Northumbria University, Newcastle, UK, 2017
[18] Rohrhuber, J., S^0 - Introducing sonification variables, in Super-Collider Symposium 2010, Berlin, pp. 1–8, 23–16 Sep. 2010.
[19] Naghshineh, K., Koopmann,G.H., Active control of sound power using acoustic basis functions as surface velocity filter, Journal of Acoustical Society of America, 93, 2740–2752, 1993.
[20] Munteanu, L., Donescu, St., Introduction to Soliton Theory: Applications to Mechanics, Book Series Fundamental Theories of Physics, vol.143, Kluwer Academic Publishers, Dordrecht, Boston, Springer Netherlands, 2004.
[21] V.Chiroiu, L.Munteanu, C.Rugină, On the control of a cooperatively robotic system by using a hybrid logic algorithm, Proceedings of the Romanian Academy, series A: Mathematics, Physics, technical Sciences, Information Science, vol.19, no.4, 2018.
[22] Hansen, C., Zidowitz, S., Ritter, F., Lange, C., Oldhafer, K., Hahn, H.K., Risk maps for liver surgery, Int. J. of Computer Assisted Radiology and Surgery, 8(3), 2012.
[23] Gheorghe, L., Iacob, S., Gheorghe, C., Real-time sonoelastography- New application in the field of liver sisease, J. Gastrointestin Liver Dis., 17(4),469-74, 2008.